nature physics

ARTICLES

PUBLISHED ONLINE: 20 JUNE 2016 | DOI: 10.1038/NPHYS3795

Dynamics of prey prehension by chameleons through viscous adhesion

Fabian Brau[1†], Déborah Lanterbecq[1†], Leïla-Nastasia Zghikh[2,3], Vincent Bels[3] and Pascal Damman[1*]

Among predators using an adhesive tongue to feed, chameleons are able to capture large prey by projecting the tongue at high acceleration. Once in contact with a prey, the tongue retracts with a comparable acceleration to bring it to the mouth. A strong adhesion between the tongue tip and the prey is therefore required during the retraction phase to ensure a successful capture. To investigate the mechanism responsible for this strong bond, the viscosity of the mucus produced at the chameleon's tongue pad is measured, using the viscous drag exerted on rolling beads by a thin layer of mucus. Here we show that the viscosity of this secretion is about 400 times larger than that of human saliva. We incorporate this viscosity into a dynamical model for viscous adhesion, which describes the motion of the compliant tongue and the prey during the retraction phase. The variation of the maximum prey size with respect to the chameleon body length is derived, and compared with *in vivo* observations for various chameleon species. Our study shows that the size of the captured prey is not limited by viscous adhesion, owing to the high mucus viscosity and large contact area between the prey and the tongue.

Chameleons are ambush opportunistic predators feeding on a large variety of invertebrate and vertebrate animals, ranging from ants to lizards[1]. They remain motionless, hidden from their own predators, and wait for active prey to come within the reach of a strike. They have developed a highly specialized feeding system based on the ballistic projection of the tongue as far as one to two body lengths with accelerations ranging from 300 to 1,500 m s^{-2}, depending on the specimen size[2–6]. This apparatus is combined with a very efficient adhesion allowing the capture of prey weighing up to 30% of their own weight[7]. The ability to project the tongue with such high acceleration has been fairly well understood[5], but the dynamics of the capture and the mechanism responsible for the strong adhesion between the prey and the tongue remains unclear. Interlocking, where the roughness of both prey and tongue surfaces self-adjust to make physical crosslinks[1,8], and a suction mechanism, similar to the one at play in rubber suction pads[9], have been proposed to supplement viscous (Stefan) adhesion[10,11]. Here we show that the ability of a chameleon tongue to ensure a close and large contact with prey, thanks to its active deformation during a capture[9], combined with a high mucus viscosity on its tip make viscous adhesion particularly efficient to capture large prey.

The viscosity of the mucus secreted at the chameleon's tongue pad is a crucial parameter to study the adhesion mechanism. However, this specific fluid is produced in very small amounts by glands in the tongue pad, and its rheology at present remains completely unknown[1]. In contrast, the rheological properties of the gastropod pedal mucus is well documented[12,13]. This highly viscous mucus ($\eta \sim 10$ Pa s) is a yield stress fluid characterized by a small yield stress ($\sim$100 Pa). It thus behaves as a soft elastic solid only when the applied stress is smaller than the yield stress and, otherwise, flows as a viscous fluid. The elastic stresses involved during a prey capture largely overcome such a yield stress (see Supplementary Information).

To obtain the viscosity of the mucus, the drag exerted by viscous forces on small steel beads rolling on a thin film of mucus is used to measure indirectly the viscosity[14]. The mucus is collected from the contact between the tongue pad and a microscope slide placed in front of a prey to provoke a shoot of the tongue. The slide is then placed without delay on a support tilted at an angle θ where the motion of a bead rolling down the slide is recorded with a camera (250 fps). As shown in Fig. 1, after a short transient stage, the bead moves at constant velocity, v_c, which is determined by θ, the fluid and the bead properties as follows

$$v_c = C_v\,(\gamma/\eta)\,(\sin\theta)^{\alpha}\left(\rho_b g R^2/\gamma\right)^{\beta}(R/h_s)^{1/2} \qquad (1)$$

The quantities $\gamma \simeq 70$ mN m^{-1}, η and h_s are the surface tension, viscosity and thickness of the mucus layer, respectively. ρ_b and R are the density and radius of the bead. g is the gravitational acceleration, $\alpha = 1.6 \pm 0.06$ and $\beta = 1.35 \pm 0.05$ are numerical constants determined experimentally[14]. $C_v = 0.014$ is the relevant value to be used in our case because the capillary number ($\eta v_c/\gamma \sim 0.04$) is much smaller than 1 (ref. 14). The validity of the method was checked with fluids of known viscosity (see Supplementary Information). The various measurements of the bead motion reported in Fig. 1 yield comparable velocities, indicating that the fluid parameters, and in particular h_s, were similar in all experiments. They do not show any evidence of an elastic behaviour of the mucus. From equation (1), the viscosity is found to lie in the range $\eta = 0.4 \pm 0.1$ Pa s, which is much larger than that of human saliva ($\sim 10^{-3}$ Pa s; ref. 15). The relatively large error is related to the uncertainty about the thickness of the mucus layer, $h_s = 25 \pm 10$ µm, which was determined by weighing and measuring the area of the film.

This unexpectedly large mucus viscosity strongly suggests that the prey sticks to the chameleon's tongue through viscous adhesion.

[1]Laboratoire Interfaces & Fluides Complexes, Université de Mons, B-7000 Mons, Belgium. [2]Laboratoire d'Histologie, Université de Mons, B-7000 Mons, Belgium. [3]Institut de Systématique, Evolution, Biodiversité, ISYEB, UMR 7205 CNRS MNHN UPMC EPHE, Muséum national d'histoire naturelle, Sorbonne Universités, CP 50, 45 rue Buffon, 75005 Paris, France. †Present addresses: Université Libre de Bruxelles (ULB), Nonlinear Physical Chemistry Unit, CP231, 1050 Brussels, Belgium (F.B.); Laboratory of Biotechnology & Applied Biology, HEPH-Condorcet & CARAH asbl, 11 rue Paul Pastur, B-7800 Ath, Belgium (D.L.). *e-mail: pascal.damman@umons.ac.be

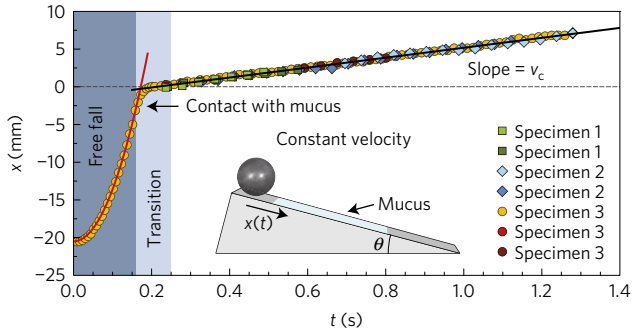

Figure 1 | Position as a function of time of a spherical steel bead rolling down an inclined plane covered by a mucus layer of thickness h_s for three specimens of *Chamaeleo calyptratus*. A free fall motion, shown only for one sequence for clarity, is followed by a regime at constant velocity, $v_c = (6.58 \pm 0.06)$ mm s^{-1}, once the bead is in contact with the fluid. The mass of the bead is $m_b = 0.175$ g ($R = 1.75$ mm and $\rho_b = 7,795$ kg m^{-3}).

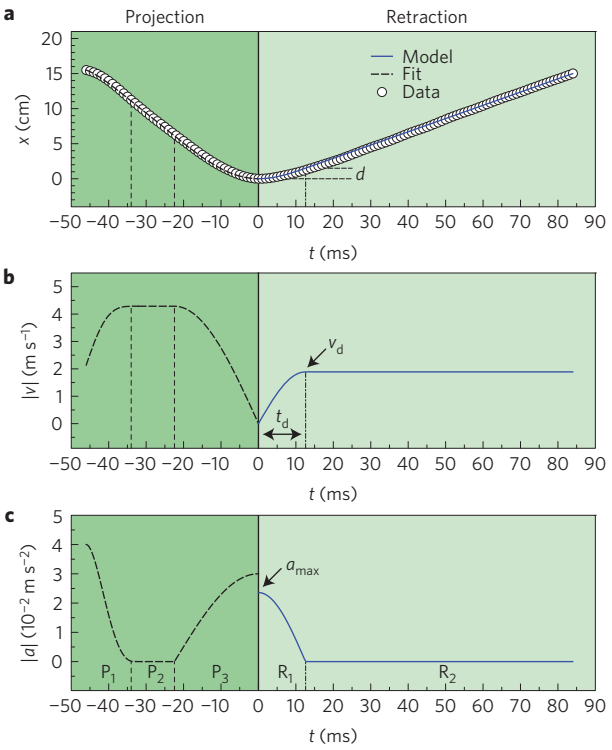

Figure 2 | Kinematics profiles for one representative capture of a cricket ($m_p \simeq 0.5$ g) by a *Chamaeleo calyptratus* specimen ($L_{SVL} = 150$ mm) recorded with a high-speed camera at 1,000 fps. a, Position of the tip of the chameleon tongue with respect to the snout position as a function of time ($t = 0$ corresponds to the onset of retraction). The curve obtained from the model (2)-(4) using the mean value of all parameters together with $k = 212\,L_{SVL}$ and $d = 0.1\,L_{SVL}$ is also shown. The projection phase has been fitted qualitatively by a piecewise polynomial function to illustrate the relevant regimes discussed in the text. d is the distance over which the acceleration is significant during the retraction phase. **b**,**c**, Velocity (**b**) and acceleration (**c**) as a function of time obtained from the model (retraction) and the fit (projection), where some relevant quantities of the retraction phase are indicated. The vertical dashed lines define the various regimes of the prey capture (see text).

However, knowing the value of this quantity is not sufficient to determine the adhesion strength. The strain/shear rate in the fluid film, which is only significant during the retraction phase, should also be known to determine the magnitude of the viscous forces[10,11]. For this purpose, we introduce a dynamical model for the retraction phase.

Figure 2 shows typical kinematics data of a prey capture recorded with a high-speed camera (1,000 fps), featuring two main phases: tongue projection and retraction. The chameleon first estimates the distance while the tongue slowly protrudes out of the jaws[16]. Then, the accelerator muscle contracts radially to squeeze against the entoglossal process of the hyoid skeleton, which leads to the projection of the tongue with a high acceleration[5,17,18]. The acceleration decreases sharply (P_1 regime) to almost vanish, such that the tongue moves at a roughly constant velocity (P_2 regime)[3,5]. The tongue then decelerates, its elongation approaching the maximal extension, and hits the prey before stopping when the velocity vanishes and the acceleration reaches a local extremum (P_3 regime). The tongue retraction then starts, with a retraction force of roughly 1 N (ref. 19), the velocity increases while acceleration decreases, and finally almost vanishes (R_1 regime). The remainder of the tongue retraction phase is performed at essentially constant velocity (R_2 regime).

This typical sequence shows that, after the tongue whips out the mouth at high acceleration, it moves essentially at roughly constant velocity except near the retraction point[5,9]. Therefore, the tongue does not behave like a stretched elastic material over its whole elongation, but only in a small region around the capture point. This is consistent with the observation that the tongue is made of nested sheaths sliding along one another like the tubes of an extending telescope[5]. Stretching occurs only once this telescopic structure has been fully deployed. To describe the retraction phase, we thus model the tongue as a spring of stiffness k stretched over a distance d which is only a fraction of the prey–jaws distance (see Supplementary Information for the case of a constant retraction force).

The retraction phase is described by considering a prey of mass m_p at a position x_p attached by a viscous fluid of thickness h to a tongue of mass m_t and position x_t. A force f_t retracts the tongue and produces a sudden increase of the mucus thickness ($dh/dt \equiv \dot{h} > 0$), inducing a viscous force f_a acting on both the tongue and the prey (see Fig. 3a). This force is due to the Poiseuille flow that is created in an incompressible viscous fluid when it deforms: $f_a = (3/2\pi)\eta\Omega^2\dot{h}h^{-5}$, where Ω is the (constant) fluid volume[10,11]. This time-dependent force features two opposite effects. At the onset of retraction, the rate of thickness variation, $\dot{h}$, induces a sharp increase of the adhesive force, which reaches a maximum value comparable to the retraction force. However, at longer time, the adhesive force vanishes due to this increase in thickness, which impacts f_a through the strong dependence h^{-5}. The rate of thickness variation is also determined by the prey mass. Moving heavier prey requires larger f_a, that is, larger $\dot{h}$, which in turn induces a sharper decrease of the adhesive force reducing the detachment time. These mechanisms explain the existence of a maximum prey mass.

To obtain this maximum prey mass quantitatively, we solve the following equations of motion

$$m_t\ddot{x}_t = f_t - f_a = k(d + h_0 - x_t)\,\mathcal{H}(d + h_0 - x_t) - \alpha\dot{h}h^{-5} \quad (2)$$

$$m_p\ddot{x}_p = f_a = \alpha\dot{h}h^{-5}, \quad \alpha = 3\eta\Sigma^2h_0^2/2\pi \quad (3)$$

$$h = x_t - x_p \quad (4)$$

with the initial conditions $x_p(0) = \dot{x}_p(0) = \dot{x}_t(0) = 0$ and $x_t(0) = h_0$ (see Supplementary Information for the role of gravity or the

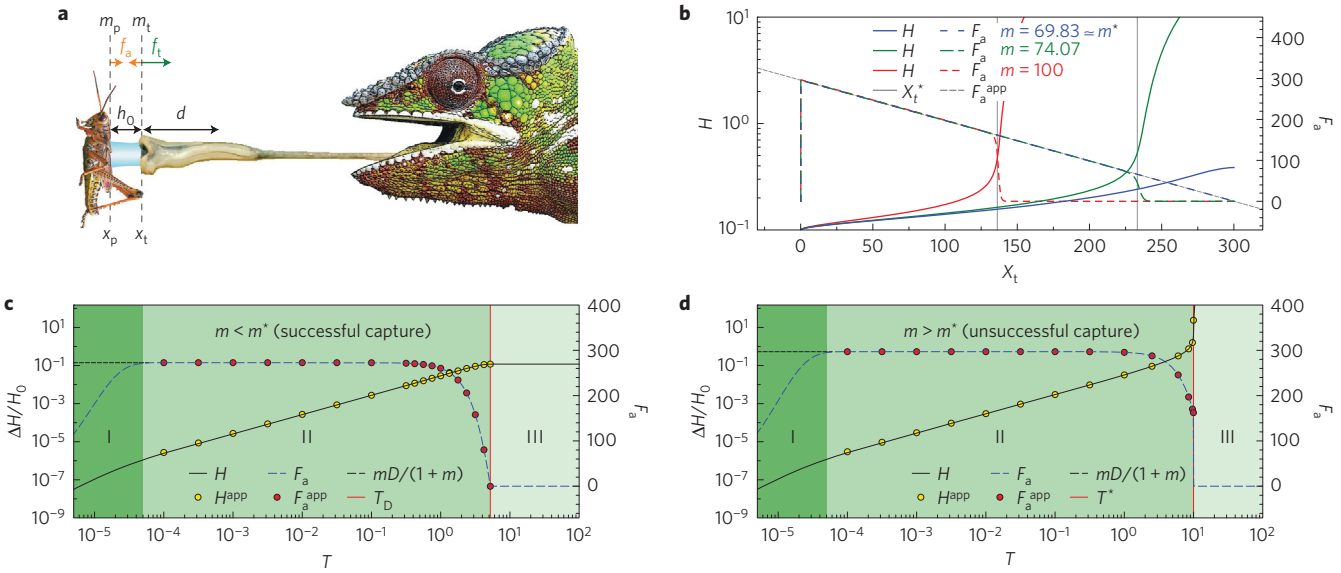

Figure 3 | Schematic of the system and results of the dynamical model. a, Schematic of the initial state of the retraction phase with the adhesion force f_a, the applied force f_t, the initial thickness of the mucus layer h_0 and the distance d over which the retraction force applies. **b**, Dependence of the normalized mucus thickness H and adhesive force F_a on the normalized position of the tongue tip X_t obtained by solving equations (5)–(7) numerically for $H_0=0.1$, $D=300$ and several values of $m=m_p/m_t$. **c**,**d**, Dependence of the relative variation of H and F_a on the normalized time T for $H_0=0.1$, $D=300$ and $m=10$ (**c**) or $m=100$ (**d**) showing three regimes: (I) onset of retraction, (II) retraction without detachment ($\Lambda=2.76$) (**c**) or with detachment ($\Lambda=0.84$) (**d**) and (III) inertial motion. The approximate expressions (8), (11) and (12) for F_a and H are also shown.

direction of the applied force with respect to the horizontal). $\Sigma=\Omega/h_0$ is the initial contact area between the prey and the tongue and h_0 is the initial mucus thickness. The influence of the tongue curvature, $1/R_t$, on the viscous flow is neglected, since $h/R_t \ll 1$. The Heaviside function $\mathcal{H}(x)$ is added to describe an applied (retraction) force vanishing when the tongue has reached a retraction distance d (that is, when $x_t > d+h_0$). Therefore, beyond that distance, only inertia is involved, h stays constant, and both the tongue and the prey move at constant speed. This implies that the prey can detach only before the tongue reaches the position $d+h_0$.

This system is characterized by the length scale $\ell=(\alpha^2/m_t k)^{1/10}$ and the timescale $\tau=(m_t/k)^{1/2}$, which are used to adimensionalize the equations of motion as follows

$$\ddot{X}_t = (D+H_0-X_t)\,\mathcal{H}(D+H_0-X_t) - \dot{H}H^{-5} \tag{5}$$

$$\ddot{X}_p = m^{-1}\dot{H}H^{-5}, \quad m=m_p/m_t \tag{6}$$

$$H = X_t - X_p \tag{7}$$

To illustrate the dynamics produced by this model, Fig. 3b shows the variations of H and $F_a=\dot{H}/H^5$ as a function of the tongue position X_t for some typical values of H_0 and D. Depending on the magnitude of m, two different behaviours are observed. When $m \le m^\star$, H stays finite and there is no detachment. The adhesive force F_a always vanishes precisely at $X_t=D+H_0$, where F_t cancels and H is therefore constant beyond that distance ($\dot{H}=0$). The prey then stays attached to the tongue, since both move at the same speed. However, when $m > m^\star$, H diverges at some detachment distance $X_t^\star$, leading to a sudden decrease in the adhesive force. Therefore, a detachment of the prey occurs when m is larger than a critical value $m^\star(H_0,D)$, derived analytically below.

Except from a tiny region near the onset of retraction, Fig. 3b shows that when the adhesive force is non-vanishing it satisfies in good approximation the following relation

$$F_a \simeq F_a^{app} = m(D+H_0-X_t)/(1+m) \tag{8}$$

Substituting equation (8) into equations (5) and (6) and solving the ODE leads to the tongue and prey positions as a function of time

$$X_t \simeq H_0 + D(1-\cos\omega T) \tag{9}$$

$$X_p \simeq D(1-\cos\omega T), \quad \omega=(1+m)^{-1/2} \tag{10}$$

These approximate solutions imply that H stays close to H_0 during the retraction. The correct time dependence of H can nevertheless be obtained from the adhesive force, which, using equations (8) and (9), reads

$$F_a \simeq F_a^{app} = \frac{\dot{H}}{H^5} \simeq \frac{Dm}{1+m}\cos\omega T \tag{11}$$

An integration leads to the variation of the mucus thickness as a function of time

$$H \simeq H^{app} = H_0\left[\frac{\Lambda}{\Lambda-\sin\omega T}\right]^{1/4}, \quad \Lambda=\frac{\sqrt{1+m}}{4mDH_0^4} \tag{12}$$

These approximate expressions (11) and (12) agree very well with the numerical solutions as seen in Fig. 3c,d and are valid until F_a vanishes. Interestingly, the approximate solution captures very well the divergence of H that occurs only when $\Lambda \le 1$. In such a case (unsuccessful capture), the adhesive force vanishes while the retraction force still applies to the tongue, leading to a prey detachment at time $T=T^\star$, or equivalently at $X_t=X_t^\star$, given by

$$T^\star = \frac{1}{\omega}\arcsin\Lambda, \quad X_t^\star = H_0 + D\left(1-\sqrt{1-\Lambda^2}\right) \tag{13}$$

After detachment, the prey moves at constant speed $V_p(T^\star)=(4mH_0^4)^{-1}$ while the tongue still accelerates until it reaches the position $D+H_0$, where F_t vanishes.

When $\Lambda > 1$, the mucus thickness H increases to reach a maximum value $H=H_0[\Lambda/(\Lambda-1)]^{1/4}$ (see equations (9), (12) and Fig. 3c). Therefore, the adhesive force acts on the prey until

the retraction force vanishes when the tongue reaches the position $D+H_0$ at time $T=T_D=\pi/(2\omega)$.

The necessary condition for a successful capture, $\Lambda>1$, imposes the following constraint on the prey mass: $m_p<m_p^\star=m_t/(16D^2H_0^8)$, assuming $m^\star\gg 1$. Returning to the physical variables, the maximum prey mass is therefore given by

$$m_p^\star=\rho V^\star=\frac{9}{64\pi^2}\frac{\eta^2\Sigma^4}{kd^2h_0^4} \tag{14}$$

where $\rho\simeq 1{,}050\,\mathrm{kg\,m^{-3}}$ is a typical prey density and $V^\star$ the prey volume[20]. The values of the parameters assumed to be constant are: $\eta=(0.4\pm0.1)$ Pa s and $h_0\simeq 2h_s=(50\pm10)\,\mu$m. In contrast, the morphological parameters, k, Σ and m_t depend on the snout-vent length, L_{SVL}, of the specimen. From kinematics and morphological data found in the literature for various chameleons, we get $k=(223\pm50)L_{SVL}$, $\Sigma=(2.6\pm0.4)\,10^{-3}L_{SVL}^{1.8}$ and $m_t=(0.24\pm0.04)L_{SVL}^{2.63}$ in MKS units (Supplementary Information). Therefore, we obtain the following order of magnitudes for the characteristic length and time scales: $\ell\simeq 0.3$–0.5 mm and $\tau\simeq 2$–9 ms for $L_{SVL}=50$–200 mm. We also expect d to scale linearly with L_{SVL}, $d=(0.2\pm0.1)L_{SVL}$ (Supplementary Information). Notice that equation (14) can also be obtained from a scaling approach by balancing the work of the retraction force and the prey kinetic energy (see Supplementary Information).

Using these parameter values, equation (14) can be written as a function of the chameleon body size as

$$V^{\star 1/3}=(1.2\pm0.6)\,L_{SVL}^{1.4} \tag{15}$$

in MKS units. In the literature, two studies report *in vivo* analysis of the stomach contents of a large number of chameleons to determine the mean maximum prey size in relation to the chameleon size[21,22]. Figure 4 shows a comparison between these data and equation (15). The maximum prey size estimated from the adhesion model is close but always larger than the experimental data, and follows the global trend with a similar exponent. Viscous adhesion alone is therefore largely sufficient to allow the capture of very large prey. Actually, the adhesive mechanism appears to be outsized with respect to the usual prey found in stomach contents. However, this outstanding adhesion strength allows chameleons to occasionally capture birds, lizards or mammals, when they have the opportunity. Viscous forces could also explain the reported capture of prey weighing 30% of the chameleon body mass[7]. For a specimen with $L_{SVL}=0.1$ m, for example, the lower estimate of the maximum prey mass is about 55% of the chameleon body mass. Notice that, during some captures, the maximum prey size could be lowered by a smaller contact area due to imperfect shooting or by gripping of the prey, both effects not considered here.

Considering the maximum retraction force $f_{max}=kd$, equation (14) can be rewritten as $m_p^\star\sim k\eta^2\Sigma^4/f_{max}^2h_0^4$. It may appear paradoxical that $m_p^\star$ decreases when the applied retraction force increases. However, as shown by equation (11), a larger applied force leads to a larger rate of thickness variation, $\dot h(0)\sim h_0^5 f_{max}$, which in turns yields a sharper increase of h and, therefore, a faster detachment of the prey.

Equation (14) shows that two parameters influence positively the adhesive trap: the fluid viscosity and the contact area. For the sake of comparison, if the viscosity of the chameleon tongue secretion was similar to human saliva ($\eta\simeq 10^{-3}$ Pa s), the maximum prey size would be reduced by roughly a factor of 50, making this mode of capture extremely inefficient. The shape of the tip of the chameleon tongue, which is large and forms a kind of cup during a capture due to the action of specific muscles[9], allows a drastic increase of the tongue–prey contact area, Σ. For small prey, that is, smaller than the tongue's tip size, this active deformation leads to a large embedding of the prey within the tongue, facilitating its capture. For large prey considered here, such an embedding is impossible, limiting the maximum prey size, as computed above.

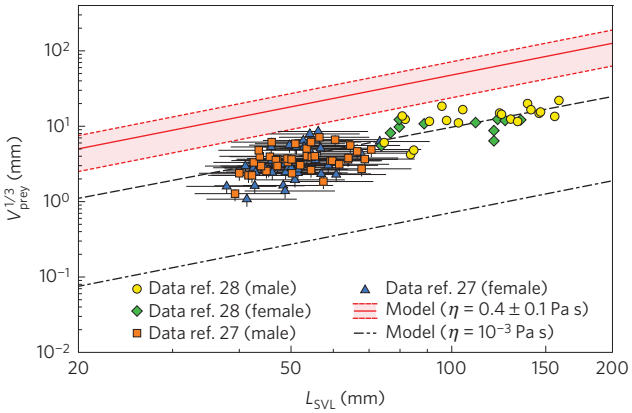

Figure 4 | Maximum prey size versus snout vent length for various chameleons. Measured maximum prey size as a function of L_{SVL} obtained for a large sampling of chameleons[21,22] plotted together with the prediction of a pure viscous adhesion model described by equation (15). The best power law fit of the data (black dashed line) leads to $V_{prey}^{1/3}\sim L_{SVL}^{1.35\pm0.08}$, with an exponent compatible with the theoretical prediction. The theoretical curve obtained with the viscosity of human saliva is shown for comparison.

Interestingly, *Plethodontidae* (salamanders) also use a ballistic tongue to capture prey, and have also developed a large and flexible tongue pad to engulf the prey and thus maximize the contact area[23,24]. Other predators also use the tongue to capture prey without resorting to ballistic projection (for example, *Bufo terrestris* (southern toad) or *Rana pipiens* (leopard frog)). It would therefore be very interesting to follow the methodology developed here, namely measuring the mucus viscosity, the contact area and the retraction force, for these specimens, to compare the predicted maximum prey size with the size of their largest prey.

Data availability. The data that support the plots within this paper and other findings of this study are available from the corresponding authors on request.

Received 13 May 2015; accepted 16 May 2016;
published online 20 June 2016

References

1. Schwenk, K. *Feeding: Form, Function, and Evolution in Tetrapod Vertebrates* (Academic, 2000).
2. Wainwright, P. C., Kraklau, D. M. & Bennett, A. F. Kinematics of tongue projection in *Chamaeleo oustaleti*. *J. Exp. Biol.* **159,** 109–133 (1991).
3. Wainwright, P. C. & Bennett, A. F. The mechanism of tongue projection in chameleons I. Electromyographic tests of functional hypotheses. *J. Exp. Biol.* **168,** 1–21 (1992).
4. Wainwright, P. C. & Bennett, A. F. The mechanism of tongue projection in chameleons, II. Role of shape change in a muscular hydrostat. *J. Exp. Biol.* **168,** 23–40 (1992).
5. de Groot, J. H. & van Leeuwen, J. L. Evidence for an elastic projection mechanism in the chameleon tongue. *Proc. R. Soc. Lond. B* **271,** 761–770 (2004).
6. Anderson, C. V. Off like a shot: scaling of ballistic tongue projection reveals extremely high performance in small chameleons. *Sci. Rep.* **6,** 18625 (2016).
7. Herrel, A., Deban, S. M., Schaerlaeken, V., Timmermans, J.-P. & Adriaens, D. Are morphological specializations of the hyolingual system in chameleons and salamanders tuned to demands on performance? *Physiol. Biochem. Zool.* **82,** 29–39 (2009).
8. Higham, T. E. & Anderson, C. V. in *The Biology of Chameleons* (eds Tolley, K. A. & Herrel, A.) 63–84 (Univ. California Press, 2013).
9. Herrel, A., Meyers, J. J., Aerts, P. & Nishikawa, K. C. The mechanics of prey prehension in chameleons. *J. Exp. Biol.* **203,** 3255–3263 (2000).

10. Stefan, J. Versuche über die scheinbare Adhäsion. *Sitz.ber. Akad. Wiss. Wien: Math. Nat.wiss. Kl.* **69,** 713–735 (1874).
11. Bikerman, J. J. The fundamentals of tackiness and adhesion. *J. Colloid Sci.* **2,** 163–175 (1947).
12. Ewoldt, R. H., Clasen, C., Hosoi, A. E. & McKinley, G. H. Rheological fingerprinting of gastropod pedal mucus and bioinspired complex fluids for adhesive locomotion. *Soft Matter* **3,** 634–643 (2007).
13. Denny, M. W. & Gosline, J. M. The physical properties of the pedal mucus of the terrestrial slug, *Ariolimax columbanus*. *J. Exp. Biol.* **88,** 375–393 (1980).
14. Bico, J., Ashmore-Chakrabarty, J., McKinley, G. H. & Stone, H. A. Rolling stones: the motion of a sphere down an inclined plane coated with a thin liquid film. *Phys. Fluids* **21,** 082103 (2009).
15. Briedis, D., Moutrie, M. F. & Balmer, R. T. A study of the shear viscosity of human whole saliva. *Rheol. Acta* **19,** 365–374 (1980).
16. Harkness, L. Chameleons use accommodation cues to judge distance. *Nature* **267,** 346–349 (1977).
17. Müller, U. K. & Kranenbarg, S. Power at the tip of the tongue. *Science* **304,** 217–219 (2004).
18. Anderson, C. V. & Deban, S. M. Ballistic tongue projection in chameleons maintains high performance at low temperature. *Proc. Natl Acad. Sci. USA* **107,** 5495–5499 (2010).
19. Herrel, A., Meyers, J. J., Aerts, P. & Nishikawa, K. C. Functional implications of supercontracting muscle in the chameleon tongue retractors. *J. Exp. Biol.* **204,** 3621–3627 (2001).
20. Matthews, P. G. D. & Seymour, R. S. Haemoglobin as a buoyancy regulator and oxygen supply in the backswimmer (Notonectidae, *Anisops*). *J. Exp. Biol.* **211,** 3790–3799 (2008).
21. Measey, G. J., Rebelo, A. D., Herrel, A., Vanhooydonck, B. & Tolley, K. A. Diet, morphology and performance in two chameleon morphs: do harder bites equate with harder prey? *J. Zool.* **285,** 247–255 (2011).
22. Kraus, F., Medeiros, A., Preston, D., Jarnevich, C. E. & Rodda, G. H. Diet and conservation implications of an invasive chameleon, *Chamaeleo jacksonii* (Squamata: Chamaeleonidae) in Hawaii. *Biol. Invasions* **14,** 579–593 (2012).
23. Deban, S. M., Wake, D. B. & Roth, R. Salamander with a ballistic tongue. *Nature* **389,** 27–28 (1997).
24. Deban, S. M., O'Reilly, J. C., Dicke, U. & van Leeuwen, J. L. Extremely high-power tongue projection in plethodontid salamanders. *J. Exp. Biol.* **210,** 655–667 (2006).

Acknowledgements

The lizard specimens were provided by C. Remy (Musée d'Histoire Naturelle de Tournai). The authors acknowledge C. Gay and D. Nonclercq for fruitful discussions. A. Maillard is acknowledged for the prey capture experiments. This work was partially supported by the MECAFOOD ARC research project from UMONS. F.B. acknowledges financial support from the Government of the Region of Wallonia (REMANOS Research Programme).

Author contributions

P.D. and V.B. conceived the study; P.D. designed the experiments; F.B., D.L., L.-N.Z. and V.B. carried out the experiments; F.B., D.L. and P.D. analysed the data; F.B. and P.D. developed the theoretical model; F.B. and P.D. wrote the manuscript.

Additional information

Supplementary information is available in the online version of the paper. Reprints and permissions information is available online at www.nature.com/reprints. Correspondence and requests for materials should be addressed to P.D.

Competing financial interests

The authors declare no competing financial interests.